Mechanics of Advanced Composite Structures 9 (2022) 243 – 262

Semnan University

Mechanics of Advanced Composite Structures

journal homepage: http://MACS.journals.semnan.ac.ir

Numerical Investigation on Free Vibration Response of Bi-Directional Porous Functionally Graded Circular/Annular Plates

D. Vasara[a], S. Khare[a*], A. Malguri[b], R. Kumar[a]

[a] *Department of Mechanical Engineering, Sardar Vallabhbhai National Institute of Technology, Surat-395007, India*
[b] *Oil and gas, HEPIPL, Adani Group, Ahmedabad – 380009, India*

KEYWORDS

Porous bi-directional functionally graded materials;
Vibration;
Circular/Annular plates;
Non-axisymmetric;
DQM.

ABSTRACT

The article presents non-axisymmetric free vibration results of porous bi-directional functionally graded (BDFG) plates. The bi-directional grading index changes with the thickness (z-) and radial (r-) directions and porosity distributions are classified as uniform or non-uniform type. A displacement field model is formulated based on First-order Shear Deformation Theory (FSDT). Hamilton's principle is used to develop the governing equations for porous BDFG plates. The spatial discretization of the proposed mathematical model in five variables is carried out using the fast converging Differential Quadrature Method (DQM). The numerous examples demonstrate the accuracy and stability of the present DQM model by comparing the reported results available in the literature. The influence of aspect ratios, boundary conditions, and porosity distributions on the free vibration response of porous bi-directional functionally graded material plates is investigated intensively. These findings reveal that increasing the porosity volume fraction significantly impacts the mechanical properties of porous bi-directional functionally graded plates.

1. Introduction

Lightweight structures are significant in aerospace, marine, nuclear, and civil engineering because new composite materials have a high strength-to-weight ratio. Lightweight isotropic and microscopically inhomogeneous functionally graded materials are made up of two or more phases with smooth material characteristics changing in specific directions. As a result, functionally graded materials can minimize inter-laminar stresses, delamination failure, and thermal deformation while also providing design ability to satisfy specific mechanical requirements.

Many authors have emphasized examining the free vibration of circular plates made up of functionally graded materials in the last decades, particularly in structural vibration. Ebrahimi and Rastgo [1] discussed the natural frequency behavior of thin functionally graded (FG) circular plates using the classical plate theory (CPT). Allahverdizadeh et al. [2] analyzed the axisymmetric vibration behavior of FG circular plate using a semi-analytical approach. Wirowski [3] studied the free vibration behavior of the FG annular plate based on the tolerance averaging technique using the Finite Difference Method (FDM).

Alipour et al. [4] studied the free vibration characteristics of the FG circular and annular plate resting on an elastic foundation with different boundary conditions. Further, The natural frequencies of thin circular FG plates resting on an elastic foundation were investigated using the differential transform method (DTM) by Shariyat and Alipour [5]. Hamzehkolaei et al. [6] used the DQM and concluded that it is an efficient and healthy numerical approach for the axisymmetric bending analysis of functionally graded circular/annular plates. Liu et al. [7] investigated the forced vibration of the FG cylindrical shell using the Pseudo-arclength continuation method. Also, Liu et al. [8] investigated the nonlinear

* Corresponding author. Tel.: +918109152818
E-mail address: sumitkhare@med.svnit.ac.in

DOI: 10.22075/macs.2022.26556.1387
Received 22-03-10; Received in revised form 22-05-05; Accepted 22-08-02

dynamic response of porous FG sandwich shells resting on the Winkler-Pasternak foundation.

Chu et al. [9] introduced the Hermite radial basis collocation method (HRBCM) to determine the natural frequencies of inhomogeneous FGM plates. Lal and Ahlawat [10] proposed a semi-analytical solution for axisymmetric vibrations of circular FGM plates using the CPT.

Li et al. [11] derived a scaling factor for modal analysis of the isotropic thin FG plate and the homogeneous FG plates using classical plate theory. Yin et al. [12] determined vibration characteristics of FG Circular plates using an isogeometric approach based on Kirchoff's plate theory. Lal and Ahlawat [13] presented the modal analysis of FG circular plate using CPT. Swaminathan et al. [14] reviewed various methods to investigate the different behavior of functionally graded plates. Merazi et al. [15] examined the static behavior of FG plates using the new hyperbolic shear deformation plate theory on neutral surface position. Arefi [16] studied the free vibration of FG circular and annular plates embedded with piezoelectric layers. Wu and Liu [17] utilized the state space-based differential reproducing kernel method (DRK) to analyze the free vibration behavior of FGMs circular/annular plates considering different boundary conditions. Żur [18] utilized the Quasi-Green function approach for investigating the free vibration behavior of the FG circular plates using CPT. Baltac [19] studied the natural frequency behavior of laminated annular/annular sector plates based on Love's shell theory and the first-order shear deformation theory. The Weak form of finite annular prism methods utilized by Wu and Yu [20] to study the static/dynamic characteristics of FG circular plates. Arshid et al. [21] investigated the natural frequency behavior of the shear deformable elastic FG plate. Javani et al. [22] presented nonlinear frequencies of elastically founded FG circular plate using Differential Quadrature Method (DQM). Singh and Azam [23] determined the natural frequencies of FGM plates, which were resting on elastic foundations under a hygro-thermal environment.

Porosity plays a significantly important role in structural specifications, and taking it into account will result in each analysis being quite similar to the experimental tests. Because of their widespread use, researchers studied the effect of the porosity of porous materials on the mechanical behavior of various structural elements such as beams, plates, and shells. Kumar et al. [24] analyzed nonlinear central deflection and stress analysis of porous FGM plates using the multiquadric radial basic function meshfree method. Mouaici et al. [25] investigated the influence of porosity distribution on the free vibration response of FGMs rectangular plates using the shear deformation plate theory. Akbaş [26] determined the natural frequency of simply-supported porous FG plate using the first-order shear deformation (FSDT) theory. Kiran and Kattimani [27] studied the porosity effect on FGM plates' free vibration characteristics using the finite element method (FEM). Barati and Zenkour [28] presented the thermo-electrical vibration behavior of piezoelectric FG plates using the refined shear deformation plate theory. Zhao et al. [29] determined the natural frequencies of thick porous FG plates with arbitrary boundary conditions on the periphery using the Fourier series method. Yousfi et al. [30] presented natural frequencies of FG porous plates using higher-order hyperbolic shear deformation plate theory. The higher-order shear deformation theory (HSDT) was utilized by Slimane [31] to investigate the natural frequencies of porous FG plates with simply supported boundary conditions. Demirhan and Taskin [32] presented a state-space-based numerical approach to analyze the effect of porosity on free vibration characteristics of FG plate using the four variable plate theory. The free vibration behavior of levy-type porous FG plates using the dynamic stiffness method was investigated by Ali and Azam [33]. Xue et al. [34] employed the isogeometric approach to determine the natural frequencies of porous FG square, rectangular and circular plates with simply supported boundary conditions using FSDT. Hadji et al. [35] predicted the influence of porosity on natural frequencies of the functionally graded rectangular plate using hyperbolic-shear deformation plate theory. Kumar et al. [36] evaluated the natural frequencies of porous FGMs rectangular plates using the inverse hyperbolic shear deformation theory. Solanki et al. [37] utilized the multi quadratic radial basic function meshfree method to investigate laminated plates' linear and nonlinear flexure analysis. The effect of porosity on the natural frequencies of Sigmoid-FGM plates was investigated by Singh and Harsha [38] using Galerkin's Vlasov Method. Balak et al. [39] determined the natural frequencies of elliptical porous sandwich plates based on CPT. Bansal et al. [40] presented Navier's solution to determine the free vibration response of FG rectangular plate having geometric discontinuities. Van Vinh and Huy [41] proposed a new hyperbolic shear deformation theory to investigate the Static and

dynamic behavior of porous FG sandwich plates using FEM.

Arshid and Khorshidvand [42] explored the free vibration behavior of porous FG circular plates using CPT. Żur and Jankowski [43] studied the influence of uniform and non-uniform porosity on the free vibration behavior of FGM Circular plates applying the CPT. Arshid et al. [44] compared the various displacement field theories for the vibration analysis of saturated porous FGM plates. Żur and Jankowski [45] presented FG porous circular plates' natural frequencies using CPT. Emdadi et al. [46] analyzed the natural frequency behavior of the circular sandwich plate using modified coupled stress theory and FSDT. Van Vinh and Tounsi [47] utilized nonlocal FSDT to investigate the natural frequencies of FG doubly curved nanoshells. Heshmati and Jalali [48] studied the free vibration response of FG porous circular/annular sandwich plate using the pseudospectral method. Amir et al. [49] investigated the free vibration behavior of FG saturated porous sandwich circular plate using modified coupled stress theory. Bennai et al. [50] presented the free vibration behavior of FG plates using higher-order hyperbolic shear deformation theory. Gao et al. [51] demonstrated a wave propagation of rectangular porous FG graphene platelets plates. Kumar and Singh [52] investigated buckling and free vibration response of the porous FGM plate using inverse hyperbolic higher-order shear deformation theory and governing equation solved by multi quadratic radial basic function meshfree method. The 3D plate theory was employed by Kaddari et al. [53] to investigate the vibrational behavior of the composite structures. Safarpour et al. [54] studied natural frequencies analysis of Functionally graded reinforced composite porous circular and annular plates using DQM. Shojaeefard et al. [55] studied the free vibration characteristics of FG porous circular plate subjected to thermal load using FSDT using the DQM method.

Many studies have been published to demonstrate and evaluate the mechanical characteristics of FGM structures. However, when material properties are distributed in various directions, axial or nonaxial FGMs are inappropriate for aeronautical applications, medical components, and higher temperature sustainable materials. The bi-directional FGMs (BDFGMs) were designed to full fill the requirements of those above-mentioned applications.

Thom et al. [56] investigated the bending and buckling response of BDFGM plates using the finite element method based on HSDT. Non-uniform rational B-spline-based material modeling was introduced by Lieu et al. [57], [58] to analyze the free vibration and buckling behavior of BDFGM rectangular plates. Hong [59] investigated natural frequencies of BDFGMs rectangular plates using FEM. Vinh [60] analyzed the bi-directional functionally graded sandwich plates using FEM based on the HSDT. Van Vinh [61] investigated the free vibration behavior of the BDFG sandwich plate on Pasternak's elastic foundation using hybrid quasi-3D theory. Many researchers have presented the free vibration response of composite materials with general boundary conditions [62] [63]. Qin et al. [64] compared a unified solution for the free vibration behavior of cylindrical shells considering arbitrary boundary conditions. using the Mindlin plate theory, Qin et al. [65] investigated the natural frequencies response of rotating cylindrical shells coupled with moderately thick annular plates. A general approach was provided by [66] to investigate the free vibration behavior of rotary FGCNT cylindrical shells considering arbitrary boundary conditions. Qin et al. [67] presented a unified solution for vibration analysis of laminated FG shallow shells with general boundary conditions using FSDT. The present study considered CC and SS boundary conditions for the particular results.

Shariyat and Alipour [68] presented the semi-analytical solution for free vibration analysis of BDFGMs circular plates resting on an elastic foundation. Tahouneh [69] studied the free vibration characteristics of BDFGMs annular plates using DQM. Lal and Ahlawat [70] utilized the CPT to determine the free vibration response of BDFGMs circular plates. Mahinzare et al. [71] analyzed the natural frequencies for BDFG piezoelectric circular plates using DQM. Shojaeefard et al. [72] investigated the free vibration characteristics of BDFG circular microplates using DQM based on FSDT. Ahlawat [73] presented a free vibration response of BDFGMs circular plate using CLPT. Molla-Alipour et al. [74] proposed the analytical formulation for natural frequencies of BDFGM annular plates by applying the differential transform method.

Numerical solutions already play a crucial role in the advancement of engineering research due to improvements in computer technology. Various numerical approaches are utilized to evaluate the solution using numerical methods, and those are regarded as effective techniques to solve the ordinary and partial differential equations (PDEs). The finite difference method (FDM), the finite volume method (FVM), the finite element method (FEM), and Galerkin and collocation methods which are types of methods of weighted residuals (MWR), are all examples of numerical simulation approaches. Among the

methodologies mentioned above, FEM and FDM are the tools that are mostly used to solve the equations. Although the most commonly used method is FEM, stress concentrations, sharp changes, singularities, and large deformation can be challenging to assess using FEM. To minimize the constraints of conventional FEM, novel approaches like wavelet-based numerical methods, mesh-free methods, the discrete singular convolution (DSC) algorithm, and other comparable techniques were developed, even if this technique overcomes the constraints of the FEM methodology. Still, these methods take very long to approximate the solution.

The differential quadrature method (DQM) is developed to eliminate some of the drawbacks of the methods mentioned above and deal with complex geometry and boundary constraints. The extra features of DQM are easy to use and capable of producing highly accurate numerical results with minimal computational effort [75]. For vibration study of a transversely isotropic hollow toroid, semi-analytical DQM was used by Jiang and Redekop [76]. Ferreira et al. [77] used the DQM approach to examine the free vibration analysis of laminated composite rectangular plates. Alibeigloo and Alizadeh [78] also utilized DQM to investigate the free vibration response of sandwich FG rectangular plates. Arani et al. [79] studied the natural frequency behavior of porous FG plates using the DQM method based on HSDT. Nejati et al. [80] utilized DQM to investigate the vibration behavior of an FG laminated rectangular plate. To prepare the in-plane natural frequencies of elastically constrained FG rectangular plates, Ji et al. [81] utilized the DQM approach.

Using the harmonic differential quadrature method, Civalek and Ulker [82] examined the bending analysis of a circular plate. Mirtalaie and Hajabasi [83] determined the natural frequency behavior of FG annular-sector plates using the DQM. Mirtalaie et al. [84] determined the natural frequencies of annular/sector FG plate using DQM. The state-space-based DQM and artificial neural network (ANN) were compared by Jodaei et al. [85] for the free vibration response of the FG sector plate. Ahlawat and Lal [86] investigated the axisymmetric vibrations of circular functionally graded plates using the generalized DQM technique. The modal analysis of rotating annular discs was accomplished by Shahriari et al. [87] using generalized DQM. Mohammadimehr et al. [88] used DQM to investigate the natural frequencies of annular/ sector FGMs plates. Lal and Saini [89] employed DQM to determine the fundamental frequencies of FG circular plates considering the thermal environment. Behravan Rad [90] investigated static analysis for porous circular BDFGMs plates using DQM. Li et al. [91] investigated the structural behavior of porous BDFGMs rectangular plates using an isogeometric approach. However, to the best of the authors' knowledge, no findings on the Bidirectional functionally graded porous circular/annular plate have been published. The porosity has a significant impact on the material's properties and strength, and it is desirable to investigate the influence of porosity on the BDFGM circular/annular plate.

The present work mainly focused on the free vibration response of bi-directional porous FGM circular and annular plates. The DQM technique is used to solve the governing equations based on the FSDT. The natural frequencies of functionally graded (FG) porous circular plates and annular plates are determined, while uniform and non-uniform porosity distributions in the thickness direction are considered. The effects of porosity distributions, porosity volume fraction, material gradation index, radius to thickness ratio, radius ratio, and boundary conditions on the free vibration response of porous bi-directional functionally graded material plates are extensively explored.

2. Mathematical Formulation

In this paper, consider BDFG porous circular/annular plates instead of unidirectional FG plates in which the material property varies in thickness and radial directions. The coordinate axis is taken at the center of the plate. The inner and outer radiuses of the plate are denoted by "*b*" and "*a*", respectively, and thickness is denoted by "*h*," as illustrated in Fig. 1.

FGMs are one type of composite material in which the mechanical properties vary continuously in the thickness direction. However, this study presents a structural analysis of FG porous circular/annular plate, whose mechanical properties vary continuously in radial and thickness directions, i.e., *r* and *z* coordinates. The Young's modulus, Poisson's ratio, and mass density of BDFGMs are expressed as:

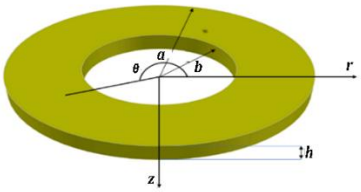

Fig.1 Annular plate

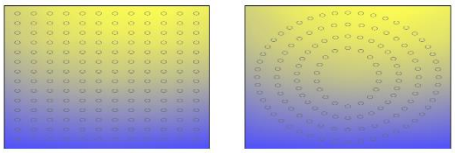

Fig. 2 Porosity distribution in the plate (uniform and non-uniform porosity distribution))

$$E = E_C\left(V_C - \frac{\delta}{2}\right) + E_m\left(V_m - \frac{\delta}{2}\right)$$
$$v = v_C\left(V_C - \frac{\delta}{2}\right) + v_m\left(V_m - \frac{\delta}{2}\right) \quad (1)$$
$$\rho = \rho_C\left(V_C - \frac{\delta}{2}\right) + \rho_m\left(V_m - \frac{\delta}{2}\right)$$

where the subscripts *m* and *c* correspond to metal and ceramic phases, V_i is the volume fraction of the internal phase, and δ stand for porosity volume fraction. The volume fraction of metal and ceramic phases phase varies in a power-law which is given as [92],

$$V_c + V_m = 1 \quad (2)$$

where,

$$V_c(r,z) = \left(\frac{1}{2} + \frac{z}{h}\right)^{n_1}\left(\frac{r}{a}\right)^{n_2}$$
$$V_m(r,z) = 1 - V_c(r,z) \quad (3)$$

Here, n_1 and n_2 are the grading indexes in thickness and radial direction. By using Eqs. (1)-(3) one can derive the effective materials properties (*P*) of the BDFG circular plate by considering two types of porosity distributions, as shown in Fig. 2 [27-29]. The material property of FGMs can be rewritten as below:

PD1: Uniform Porosity Distribution

$$P = P_m + (P_c - P_m)\left(\frac{1}{2} + \frac{z}{h}\right)^{n_1}\left(\frac{r}{a}\right)^{n_2} - \frac{\delta}{2}(P_c + P_m) \quad (4)$$

PD2:Non-uniform porosity distribution

$$P = P_m + (P_c - P_m)\left(\frac{1}{2} + \frac{z}{h}\right)^{n_1}\left(\frac{r}{a}\right)^{n_2} - \frac{\delta}{2}(P_c + P_m)\left(1 - \frac{2|z|}{h}\right) \quad (5)$$

where, *P* stands for the property of the material in which young modulus (*E*), Poisson's ratio (v), and density (ρ) are considered, P_c and P_m refer to ceramic and metal materials, respectively.

The effect of uniform and non-uniform porosity distribution on young modulus (*E*) in the thickness direction is represented in Figs. 3-4 respectively.

2.1. Governing equation of the BDFGM circular/annular plate

The displacement field for the given plate defines based on the FSDT theory. According to FSDT, displacement in *r*, θ, and *z*-direction is provided below by Akbari and Asanjarani [93]:

$$U_r(r,\theta,z,t) = u(r,\theta,t) + z\varphi_r(r,\theta,t)$$
$$U_\theta(r,\theta,z,t) = v(r,\theta,t) + z\varphi_\theta(r,\theta,t) \quad (6)$$
$$U_z(r,\theta,z,t) = w(r,\theta,t)$$

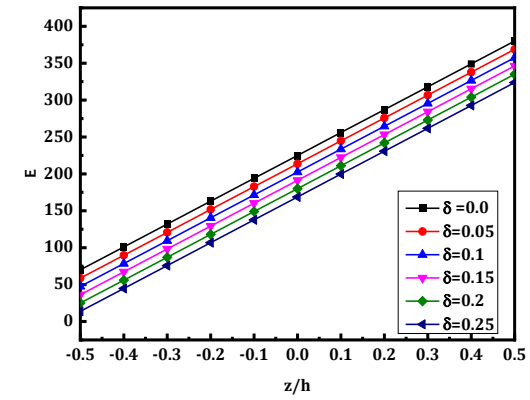

(a)

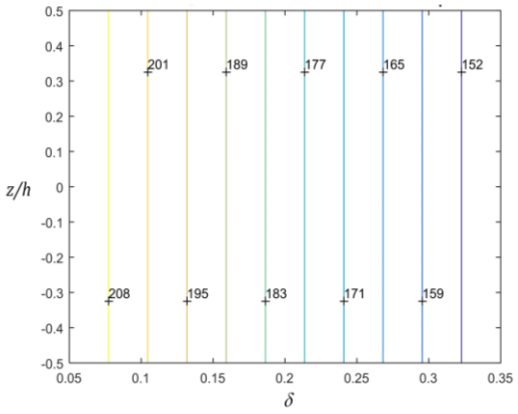

(b)

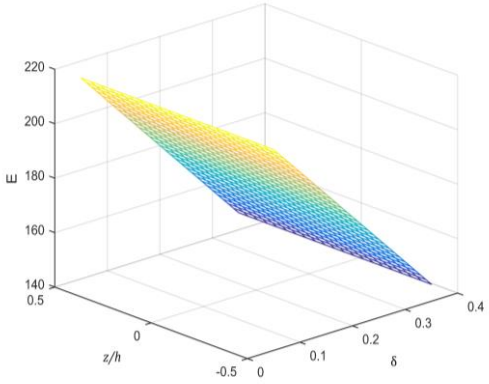

(c)

Fig. 3 (a-c) Variation of Young modulus through the thickness with different porosity volume fractions for uniform porosity distribution (n_1=1).

The above equation u,v,w denotes midplane displacement in the radial, circumferential and transverse directions, respectively, and φ_r,φ_θ are considered as rotation in *rz* and θz planes, and variable "t" represents the time.

The following are the component of strain in the displacement field in terms of mid-surface deflection and curvature effect:

$$\begin{Bmatrix} \varepsilon_r \\ \varepsilon_\theta \\ \gamma_{rz} \\ \gamma_{\theta z} \\ \gamma_{r\theta} \end{Bmatrix} = \begin{Bmatrix} \varepsilon_r^{\,0} \\ \varepsilon_\theta^{\,0} \\ \gamma_{rz} \\ \gamma_{\theta z} \\ \gamma_{r\theta}^{\,0} \end{Bmatrix} + z \begin{Bmatrix} k_r^{\,0} \\ k_\theta^{\,0} \\ 0 \\ 0 \\ k_{r\theta}^{\,0} \end{Bmatrix} \tag{7}$$

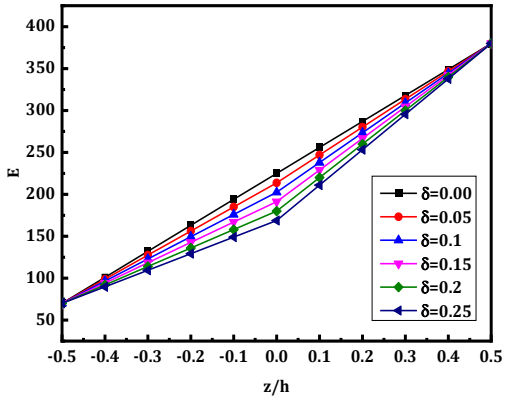

(a)

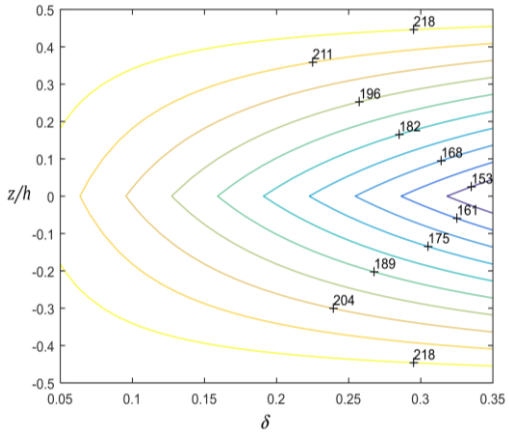

(b)

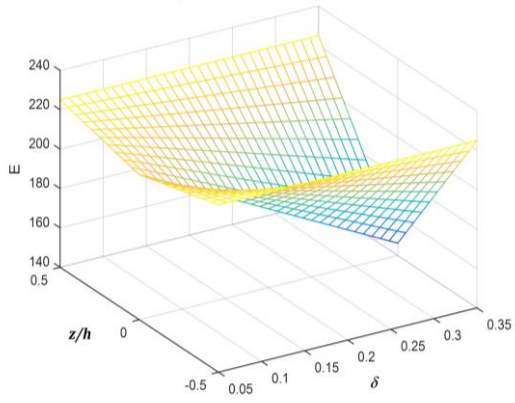

(c)

Fig. 4 (a-c) Variation of Young modulus through the thickness with different porosity volume fractions for non-uniform porosity distribution (n_1=1).

The above Eq. (7) $\varepsilon_r, \varepsilon_\theta, \gamma_{r\theta}$ are the normal strains in the respective directions and $\gamma_{\theta z}$ γ_{rz} are transverse strains in the respective directions.

Further terms of Eq. (7) are explored as below:

$$\begin{Bmatrix} \varepsilon_r^{\,0} \\ \varepsilon_\theta^{\,0} \\ \gamma_{rz} \\ \gamma_{\theta z} \\ \gamma_{r\theta}^{\,0} \end{Bmatrix} = \begin{Bmatrix} u_{,r} \\ \frac{1}{r}(u + v_{,\theta}) \\ \varphi_\theta + \frac{1}{r} w_{,\theta} \\ \varphi_r + w_{,r} \\ \frac{1}{r}(u_{,\theta} - v) + v_{,\theta} \end{Bmatrix} \& \begin{Bmatrix} k_r^{\,0} \\ k_\theta^{\,0} \\ 0 \\ 0 \\ k_{r\theta}^{\,0} \end{Bmatrix} = \begin{Bmatrix} \varphi_{r,r} \\ \frac{1}{r}(\varphi_r + \varphi_{\theta,\theta}) \\ 0 \\ 0 \\ \frac{1}{r}(\varphi_{r,\theta} - \varphi_\theta) + \varphi_{\theta,\theta} \end{Bmatrix} \tag{8}$$

where,

$u_{,r} = \frac{\partial u}{\partial r}$, $u_{,\theta} = \frac{\partial u}{\partial \theta}$, $v_{,\theta} = \frac{\partial v}{\partial \theta}$. $w_{,\theta} = \frac{\partial w}{\partial \theta}$,

$w_{,r} = \frac{\partial w}{\partial r}$, $\phi_{r,r} = \frac{\partial \phi_r}{\partial r}$, $\phi_{r,\theta} = \frac{\partial \phi_r}{\partial \theta}$, $\phi_{\theta,\theta} = \frac{\partial \phi_\theta}{\partial \theta}$, and

$\phi_{\theta,r} = \frac{\partial \phi_\theta}{\partial r}$.

In the displacement field of the FGM plate, in-plane resultant forces ($N_r, N_\theta, N_{r\theta}$), in-plane resultant moment ($M_{rr}, M_{\theta\theta}, M_{r\theta}$), and shear forces ($Q_r, Q_\theta$) are given by the equation below[94].

$$\begin{Bmatrix} N_r \\ N_\theta \\ N_{r\theta} \\ M_{rr} \\ M_{\theta\theta} \\ M_{r\theta} \end{Bmatrix} = \begin{bmatrix} A_{11} & A_{12} & 0 & B_{11} & B_{12} & 0 \\ A_{21} & A_{22} & 0 & B_{21} & B_{22} & 0 \\ 0 & 0 & A_{66} & 0 & 0 & B_{66} \\ B_{11} & B_{12} & 0 & D_{11} & D_{12} & 0 \\ B_{21} & B_{22} & 0 & D_{21} & D_{22} & 0 \\ 0 & 0 & B_{66} & 0 & 0 & D_{66} \end{bmatrix} \begin{Bmatrix} \varepsilon_r^{\,0} \\ \varepsilon_\theta^{\,0} \\ \gamma_{r\theta}^{\,0} \\ k_r^{\,0} \\ k_\theta^{\,0} \\ k_{r\theta}^{\,0} \end{Bmatrix} \tag{9}$$

and

$$\begin{bmatrix} Q_r \\ Q_\theta \end{bmatrix} = k_s \begin{bmatrix} A_{44} & 0 \\ 0 & A_{55} \end{bmatrix} \begin{bmatrix} \gamma_{rz} \\ \gamma_{\theta z} \end{bmatrix} \tag{10}$$

In Eqs. (9) and (10), A_{ij}, B_{ij}, D_{ij} matrices stand for extensional stiffness matrix, the bending-extensional coupling stiffness matrix, and the bending stiffness matrix respectively. and k_s=5/6 refers to Shear Correction Factor [95]. A_{ij}, B_{ij}, D_{ij} matrices can be referred to Molla-Alipour et al. [74]:

$$A_{ij}=\int_{-\frac{h}{2}}^{\frac{h}{2}}Q_{ij}(r,\theta)dz \qquad \left(i,j\ =\ 1,2,4,5,6\right)$$

$$B_{ij}=\int_{-\frac{h}{2}}^{\frac{h}{2}}Q_{ij}(r,\theta)zdz \qquad \left(i,j=1,2,6\right) \tag{11}$$

$$D_{ij}=\int_{-\frac{h}{2}}^{\frac{h}{2}}Q_{ij}(r,\theta)z^2dz \quad \left(i,j=1,2,6\right)$$

In above Eq. (11), Q_{ij} is the stiffness constant for the FGM plate. Element of Q_{ij} matrix is mentioned below:

$$Q_{11}=\frac{E_1}{[1-\upsilon_{12}{}^2(E_2/E_1)]},Q_{22}=\frac{E_2}{[1-\upsilon_{12}{}^2(E_2/E_1)]},$$
$$Q_{12}=\frac{\upsilon_{12}E_2}{[1-\upsilon_{12}{}^2(E_2/E_1)]},Q_{44}=G_{23},Q_{55}=G_{13}Q_{66}=G_{12},Q_{45}=0 \tag{12}$$

In Eq. 12, the directions r, θ, and z are represented as 1, 2, and 3, respectively.

The governing equation of the FG circular/annular plate can be derived from Hamilton's principle. An analytical form of Hamilton's principle is stated below:

$$\int_0^T(\delta S_e-\delta K_e)dt=0 \tag{13}$$

where, $\delta S_e,\delta K_e$ denotes variation in strain energy and kinetic energy, respectively. Using Hamilton's principle, five equations of motion in terms of the stress resultants can be written as below:

$$\delta u:\frac{1}{r}\left(\frac{\partial N_r}{\partial\theta}-N_\theta+N_r\right)+\frac{\partial N_r}{\partial r}=I_1\frac{\partial^2\varphi_r}{\partial^2t}+I_0\frac{\partial^2u}{\partial^2t} \tag{14}$$

$$\delta v:\frac{1}{r}\left(2N_{r\theta}+\frac{\partial N_\theta}{\partial\theta}\right)+\frac{\partial N_{r\theta}}{\partial r}=I_1\frac{\partial^2\varphi_\theta}{\partial^2t}+I_0\frac{\partial^2v}{\partial^2t} \tag{15}$$

$$\delta w:\frac{1}{r}\left(Q_r+\frac{\partial Q_\theta}{\partial\theta}\right)+\frac{\partial Q_r}{\partial r}=I_0\frac{\partial^2w}{\partial^2t} \tag{16}$$

$$\delta\varphi_r:\frac{\partial M_r}{\partial r}+\frac{1}{r}\left(\frac{\partial M_{r\theta}}{\partial\theta}+M_r-M_\theta\right)-Q_r=I_1\frac{\partial^2u}{\partial^2t}+I_2\frac{\partial^2\varphi_r}{\partial^2t} \tag{17}$$

$$\partial\varphi_\theta:\frac{1}{r}\left(2M_{r\theta}+\frac{\partial M_\theta}{\partial\theta}\right)+\frac{\partial M_{r\theta}}{\partial r}+-Q_\theta=I_1\frac{\partial^2v_0}{\partial^2t}+I_2\frac{\partial^2\varphi_\theta}{\partial^2t} \tag{18}$$

where I_1 and I_2 stand for mass moment of inertia which defines below:

$$\left(I_0,I_1,I_2\right)=\sum\int_{-h/2}^{h/2}\rho\left(1,z,z^2\right)dz \tag{19}$$

2.2. Boundary Condition and Method of Solution

Bellman and his colleagues [96] introduced the DQM in 1972. The DQM method is mostly used to solve ordinary and partial differential equations. The basic idea about DQM is based on the guess quadrature integration method. It may be effectively stated extending the guess quadrature to evaluate the higher-order derivatives of differentiable function gives rise to DQM. In simple words, derivatives of various order can be found by weighted linear sums of the function values at all grid points inside the domain. As discussed in the literature, the DQM is theoretically simple, and it produces very accurate solutions with less computational effort.

The solution domain is divided into several points r_i (i = 1, 2,..., N). The p^{th}-order derivative of transverse displacement with respect to r at point r_i (with M divisions in that r-direction) is approximated by [97]:

$$\left.\frac{\partial^p\phi}{\partial r^p}\right|_i=\sum_{k=1}^{M}B_{rik}^{(p)}\psi_k \tag{20}$$

- $B_{rik}^{(p)}$ is the p^{th} order derivative weighting coefficient of the function ϕ at the i^{th} point in the space domain.
- ψ_k is the function value at the i^{th} point in the space domain.

The weighting coefficients $B_{rik}^{(p)}$ can be calculated using the recurrence relations [97],

$$B_{rik}^{(p)}=\mathrm{p}\left(B_{rii}^{(p-1)}B_{rik}^{1}-\frac{B_{rik}^{(p-1)}}{\left(\mathrm{r_i}-\mathrm{r}_k\right)}\right) \tag{21}$$

where i = 1, 2, . . ., M, k = 1, 2, . . ., M with $i \neq k$, and , p = 1, 2, ...M – 1.

$$B_{rik}^{(p)}=-\sum_{k=1,k\neq i}^{M}B_{rik}^{(p)} \tag{22}$$

where i = 1, 2,. . ., M with p = 1, 2,. . .. M – 1

$$B_{rik}^{1}=\frac{\prod_{j=1,j\neq i}^{M}\left(r_i-r_j\right)}{\left(r_i-r_k\right)\prod_{j=1,j\neq i}^{M}\left(r_k-r_j\right)} \tag{23}$$

where i= 1, 2,. . ., M , k = 1, 2,. . ., M with $i \neq k$.

The cosine rule is used to create grid point coordinates.

$$r_m=\frac{(a-b)}{2}\left\{1-\cos\left[\frac{(m-1)\pi}{M-1}\right]\right\}+b \tag{24}$$

for m = 1, 2,. . ., M.

The gridpoint distribution on the peripheral (theta) direction is obtained using the following relation for m= 1, 2,..., N.

$$\theta_m=\frac{\theta}{2}-\frac{\theta}{2}\cos\left[\frac{\left(m-1\right)\pi}{M-1}\right] \tag{25}$$

The elastic boundary conditions are considered along the edge of the FGM plate are as follows:

$$\begin{aligned} k_{uj}u + N_r &= 0 \\ k_{vj}v + N_{r\theta} &= 0 \\ k_{wj}w + Q_r &= 0 \\ k_{\phi_\theta j}\varphi_\theta + M_{r\theta} &= 0 \\ k_{\phi_r j}\varphi_r + M_r &= 0 \end{aligned} \tag{26}$$

The stiffness constants k_{ij} ($i = u,v,w,\varphi_r,\varphi_\theta$ and j = 1, 2, 3, 4) for the respective displacements at the four boundaries (j = 1 for $r = b$, j = 2 for θ = 0, j = 3 for $r = a$ and j = 4 for $\theta = \Theta$) are shown in Fig. 5.

Using the formulation described above, one algebraic equation is obtained for each displacement component at each domain. These equations are derived from either an equilibrium equation or a boundary condition. The following eigenvalue problems were derived from the resulting set of algebraic equations.

$$\left(\left[K\right] - \omega^2\left[M\right]\right)q_b = 0 \tag{27}$$

Here, for example, the vector q_b contains the amplitudes for the displacement component. MATLAB software is used to calculate natural frequencies from the eigenvalue equation specified by Eq. (27).

3. Numerical Results and Discussion

This work presents the free vibration responses of BDFG circular and annular plates with thickness "*h*", outer radius "*a*", and inner radius *"b"*. The circular/annular plates examined in this article are made of two distinct material sets. The material properties of these two sets of material for the BDFG circular/annular plates are reported in Table 1.

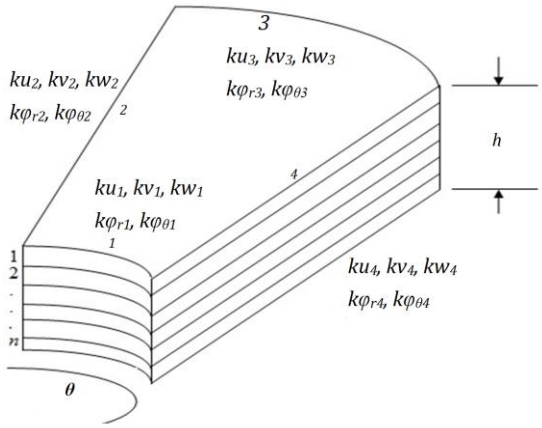

Fig. 5. Stiffness constants along the radial and circumferential edges

Table 1. Functionally Graded Material Property

Property	Material 1 [12]		Material 2 [45]	
	Si_3N_4	SUS304	Al	Al_2O_3
E(GPa)	348.43	201.04	70	380
v	0.24	0.3262	0.3	0.3
ρ(kg/m3)	2370	8166	2707	3800

The non-dimensional elastic foundation coefficients are defined as:

$$\overline{k_{i,j}} = \frac{k_{i,j}a^3}{D_{22}} \forall\, i = u,v,w; j = 1,3 \tag{28}$$

$$\overline{k_{i,j}} = \frac{k_{i,j}a}{D_{22}} \forall\, i = \varphi_r,\varphi_\theta; j = 1,3 \tag{29}$$

$$\overline{k_{I,J}} = \begin{bmatrix} \overline{k_{u,1}} & \overline{k_{u,3}} \\ \overline{k_{v,1}} & \overline{k_{v,3}} \\ \overline{k_{w,1}} & \overline{k_{w,3}} \\ \overline{k_{\varphi_r,1}} & \overline{k_{\varphi_r,3}} \\ \overline{k_{\varphi_\theta,1}} & \overline{k_{\varphi_\theta,3}} \end{bmatrix} \tag{30}$$

Thus, considering an annular plate with both edges clamped (CC),

$$\overline{k_{i,j}} = [10^{12},10^{12},10^{12},10^{12},10^{12};10^{12},10^{12},10^{12},10^{12},10^{12}]^T, \tag{31}$$

and for an annular plate with both edges simply supported (SS),

$$\overline{k_{i,j}} = [10^{12},10^{12},10^{12},0,10^{12};10^{12},10^{12},10^{12},0,10^{12}]^T \tag{32}$$

3.1. Convergence and validation study

In order to demonstrate the validation of the present DQ method, firstly, consider a homogeneous circular plate with clamped and simply supported boundary conditions. The circular plate made up of Material 1 with outer radius (*a)* = 1.0 m, radius to thickness ratio (*a/h)* = 100. In Fig. 6., the numerical results are compared to analytical solutions [9], the Hermite radial basis collocation method (HRBCM) [9], and the isogeometric approach (IGA) [12] with respect to the number of nodes in the radial (M) and circumferential (N) directions. The normalized natural frequency is considered as $\Omega = \omega a^2\sqrt{\rho h / D_0}$ where $D_0 = E_c h^3 / 12(1-v^2)$. It is observed that the results obtained by DQM are in good agreement at (*M*x*N*=14x12) with the analytical solutions, HRBCM and IGA.

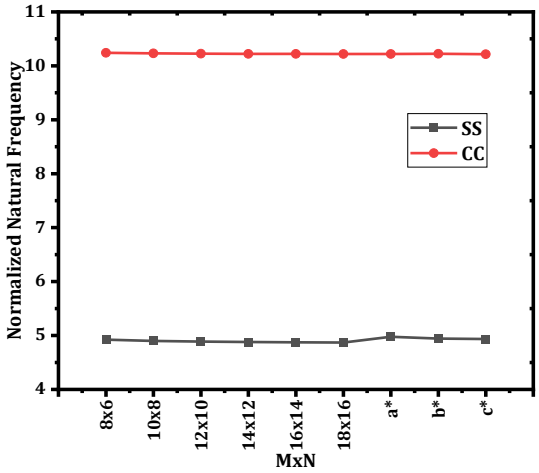

Fig. 6. Convergence study on normalized natural frequencies of the isotropic circular plate for clamp and simply supported boundary condition
*a,*b: Chu et al. [9]; *c: Yin et al. [12]

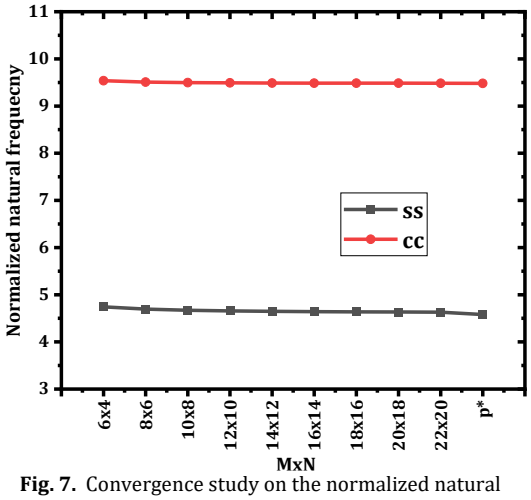

Fig. 7. Convergence study on the normalized natural frequency of FGM circular plate in z-direction for clamp and simply-supported boundary condition
*p: Żur and Jankowski [45]

Fig. 7. depicts the convergence and comparison studies for grading index in the thickness direction (n_1=0.2, Material 2) with Żur and Jankowski [45] considering clamp (CC) and simply supported (SS) boundary condition. The plate is made up of Material 2. The fundamental frequencies agree in the range of 2%, at (M x N =14x12).

Tables 2 and 3 demonstrate the convergence results compared to the results of Yin et al. [12] for the first four modes normalized frequencies in the account of different gradient indexes in the thickness direction (n_1), considering both simply supported and clamped boundary condition. The result is obtained by taking the material property of the plate as material 1 with thickness to radius ratio (h/a)=0.01 and grading index in the radial direction (n_2)=0. It is observed that the results obtained by DQM are in good agreement at (MxN=14x12) with the Yin et al. [12] for clamped and simply-supported FGM circular plates.

3.2. Parametric Study

After validating the present formulation, the results of certain parametric studies are conducted to discuss the effect of various porosity distributions (uniform and non-uniform distribution), porosity volume fraction, radius to thickness ratio (a/h), material gradation index (thickness direction (n_1), and radial direction(n_2)), radius ratio (b/a), and boundary conditions on normalized natural frequencies of porous bi-directional FG plates.

3.2.1. Influence of porosity distribution

The influence of different porosity distributions, such as uniform (PD1) and non-uniform (PD2) porosity distribution, on normalized natural frequency parameters, is shown in Figs. 8-9 for both simply supported and clamped boundary conditions with Material 1. The material grading index in thickness direction (n_1) and in radial direction (n_2) are considered as (n_1,n_2)=(2,0), (0,2), (2,2), (5,0), (0,5), (5,5)and radius to thickness ratio is taken as (a/h)=10.The normalized natural frequency parameter is considered as, $\Omega = \omega_i a^2 \sqrt{\rho h / D_c}$ where $D_c = E_c h^3 / 12(1-\nu_c^2)$.

Figs. 8 (a-b) show the effect of porosity volume fraction (δ) on normalized natural frequencies for clamped porous circular plates with uniform (PD1) and non-uniform (PD2) porosity distribution, respectively. While Figs. 9 (a)-(b) show the effect of porosity volume fraction (δ) on normalized natural frequencies for simply supported porous circular plates with uniform (PD1) and non-uniform (PD2) porosity distribution, respectively.

It is observed that for uniform porosity distribution, the natural frequency decreases with an increase in porosity volume fraction, whereas for non-uniform porosity distribution, the normalized natural frequency increase with the increase in porosity volume fraction for both the clamped and simply supported boundary condition. It is also observed that natural frequency parameters in case of BDFG plates ((n_1,n_2)= (2,2), (5,5)) are less than unidirectional FG plates(n_1,n_2)=(2,0), (0,2), (5,0), (0,5) for both the clamped and simply supported boundary condition.

Table 2. Convergence and comparison study on the normalized natural frequency of simply supported FGM circular plate with various grading indexes (n_1) in the thickness direction

*M*x*N*	Mode No.	Grading index (n_1)					
		0	0.5	1	2	5	8
Yin et al.[12]	1	4.8448	3.3379	2.856	2.4831	2.2177	2.1584
	2	13.8243	10.2762	8.7858	7.4588	6.3758	6.1147
	3	13.8243	10.2762	8.7858	7.4588	6.3758	6.1147
	4	25.5513	19.7272	16.9998	14.4161	12.103	11.4768
8x6	1	4.9225	3.4317	2.9956	2.6539	2.3719	2.2879
	2	14.161	9.8192	8.5437	7.5385	6.7081	6.46
	3	14.283	9.9034	8.617	7.6032	6.7658	6.5155
	4	26.324	18.237	15.859	13.985	12.436	11.972
10x8	1	4.8996	3.4153	2.9813	2.6402	2.3595	2.2756
	2	14.336	9.9416	8.6506	7.6333	6.7931	6.542
	3	14.354	9.9538	8.6612	7.6427	6.8014	6.55
	4	25.852	17.913	15.579	13.739	12.218	11.764
12x10	1	4.8876	3.4059	2.9722	2.6323	2.3521	2.2687
	2	14.386	9.9772	8.6823	7.662	6.8193	6.5675
	3	14.387	9.9777	8.6826	7.6624	6.8196	6.5678
	4	25.568	17.716	15.407	13.588	12.084	11.634
14x12	1	4.8787	3.4002	2.9674	2.6274	2.3475	2.2641
	2	14.433	10.011	8.7127	7.6895	6.8446	6.5921
	3	14.433	10.011	8.7127	7.6895	6.8446	6.5922
	4	25.57	17.717	15.408	13.588	12.084	11.634
16x14	1	4.8744	3.3962	2.9638	2.624	2.3442	2.261
	2	14.477	10.043	8.7412	7.7155	6.8686	6.6154
	3	14.478	10.043	8.7413	7.7156	6.8686	6.6154
	4	25.572	17.718	15.409	13.588	12.084	11.634
18x16	1	4.8698	3.3926	2.9605	2.6213	2.3422	2.2588
	2	14.52	10.074	8.7689	7.7408	6.8918	6.6382
	3	14.52	10.074	8.769	7.7409	6.8918	6.6382
	4	25.567	17.714	15.405	13.585	12.081	11.631

Table 3. Convergence and comparison study on the normalized natural frequency of clamped FGM circular plate with various grading indexes in the thickness direction

*M*x*N*	Mode No.	Grading index (n_1)					
		0	0.5	1	2	5	8
Yin et al. [12]	1	10.2165	6.8437	5.9037	5.2313	4.7694	4.6408
	2	21.2715	15.2397	12.9954	11.163	9.8535	9.5662
	3	21.2715	15.2397	12.9954	11.163	9.8535	9.5662
	4	34.9104	26.008	22.2423	18.9242	16.2905	15.6824
8x6	1	10.242	7.0897	6.162	5.4303	4.8251	4.6442
	2	21.384	14.794	12.854	11.323	10.057	9.6778
	3	21.532	14.897	12.944	11.403	10.128	9.7461
	4	36.059	24.957	21.69	19.113	16.982	16.344
10x8	1	10.231	7.0813	6.1548	5.4239	4.8194	4.6387
	2	21.529	14.895	12.943	11.402	10.127	9.7456
	3	21.553	14.912	12.957	11.415	10.139	9.7567
	4	35.163	24.336	21.151	18.638	16.559	15.937
12x10	1	10.225	7.0778	6.1516	5.4208	4.8164	4.6356
	2	21.526	14.893	12.941	11.401	10.126	9.7448
	3	21.527	14.894	12.942	11.401	10.127	9.7453
	4	34.848	24.118	20.961	18.471	16.411	15.794
14x12	1	10.222	7.0755	6.1497	5.419	4.8149	4.6341
	2	21.526	14.893	12.941	11.401	10.126	9.745
	3	21.526	14.893	12.941	11.401	10.126	9.745
	4	34.86	24.187	20.969	18.477	16.416	15.8
16x14	1	10.221	7.0742	6.1483	5.4178	4.8139	4.6331
	2	21.524	14.892	12.941	11.4	10.126	9.7447
	3	21.525	14.893	12.941	11.4	10.126	9.7447
	4	34.872	24.135	20.976	18.484	16.422	15.805
18x16	1	10.219	7.0733	6.1476	5.4172	4.8131	4.6325
	2	21.523	14.892	12.94	11.4	10.126	9.7444
	3	21.523	14.892	12.94	11.4	10.126	9.7444
	4	34.872	24.135	20.976	18.484	16.422	15.806

Table 4. The normalized natural frequencies of the clamped porous FG circular and annular plate for different material grading indexes in the thickness direction

Porosity distribution	b/a	Grading index (n_1)					
		0	0.5	1	2	5	10
PD1	0	10.86	6.9058	5.9235	5.2384	4.7081	4.4548
	0.1	27.68	17.586	15.066	13.288	11.901	11.259
	0.2	34.72	22.042	18.882	16.653	14.913	14.109
	0.3	44.621	28.302	24.237	21.366	19.124	18.093
	0.5	74.364	47.321	40.04	34.424	29.829	27.968
PD2	0	10.475	6.9325	6.0061	5.3487	4.8326	4.5862
	0.1	26.65	17.625	15.249	13.543	12.192	11.567
	0.2	33.413	22.086	19.106	16.967	15.273	14.49
	0.3	42.911	28.344	24.513	21.758	19.573	18.57
	0.5	70.995	46.894	40.051	34.7	30.287	28.494

Table 5. The normalized natural frequencies of clamped porous FG circular and annular plate for different material grading indexes in the radial direction

Porosity distribution	b/a	Grading index (n_2)					
		0	0.5	1	2	5	10
PD1	0	10.86	7.0271	6.0043	5.2188	4.5794	4.3227
	0.1	27.68	17.893	15.279	13.269	11.632	10.973
	0.2	34.72	22.441	19.161	16.639	14.584	13.757
	0.3	44.621	28.833	24.614	21.37	18.725	17.661
	0.5	74.364	47.444	40.169	34.524	29.873	27.984
PD2	0	10.475	7.0428	6.0777	5.3263	4.7102	4.462
	0.1	26.65	17.902	15.438	13.517	11.939	11.302
	0.2	33.413	22.445	19.354	16.944	14.964	14.165
	0.3	42.911	28.821	24.847	21.748	19.2	18.172
	0.5	70.995	47.004	40.169	34.793	30.328	28.509

Table 6. The normalized natural frequencies of the clamped BDFG circular and annular plate with grading index in thickness and radial direction

Porosity distribution	b/a	Grading index (n_1,n_2)					
		(0,0)	(0.5,0.5)	(1,1)	(2,2)	(5,5)	(10,10)
PD1	0	10.86	5.6581	4.8634	4.4119	4.1488	4.0749
	0.1	27.68	14.402	12.359	11.192	10.517	10.333
	0.2	34.72	18.057	15.495	14.029	13.183	12.952
	0.3	44.621	23.191	19.895	18.007	16.918	16.623
	0.5	74.364	38.114	32.079	28.468	26.492	26.045
PD2	0	10.475	5.7499	4.986	4.548	4.2928	4.2218
	0.1	26.65	14.609	12.646	11.512	10.858	10.681
	0.2	33.413	18.311	15.849	14.426	13.605	13.384
	0.3	42.911	23.504	20.337	18.504	17.448	17.165
	0.5	70.995	38.219	32.449	28.975	27.071	26.64

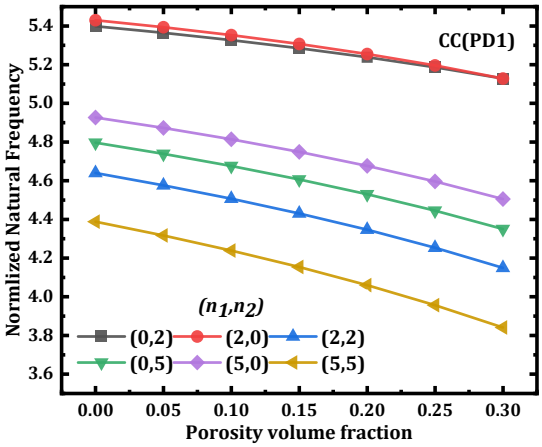

Fig. 8a. Effect of porosity volume fraction on the normalized natural frequency of clamped (CC) BDFG plates with uniform porosity distribution

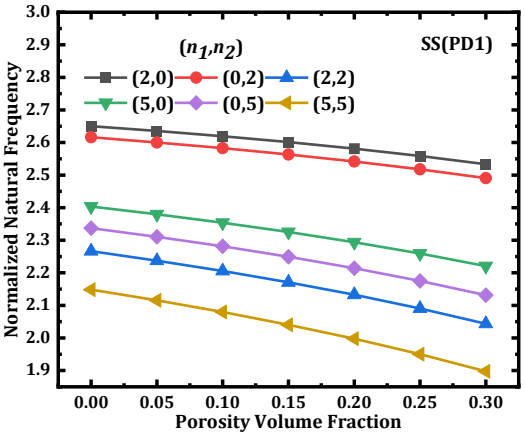

Fig. 9a. Effect of porosity volume fraction on the normalized natural frequency of simply supported (SS) BDFG plates with uniform porosity distribution

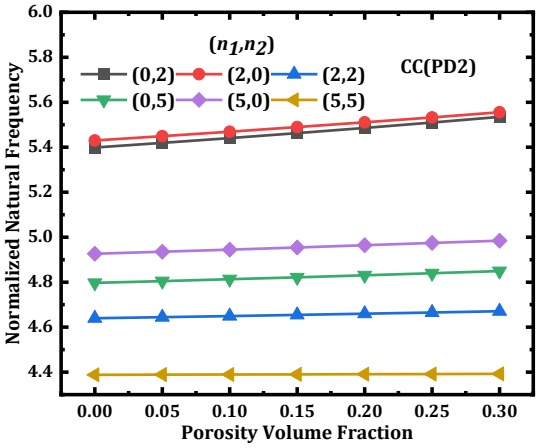

Fig. 8b. Effect of porosity volume fraction on the normalized natural frequency of clamped (CC) BDFG plates with non-uniform porosity distribution

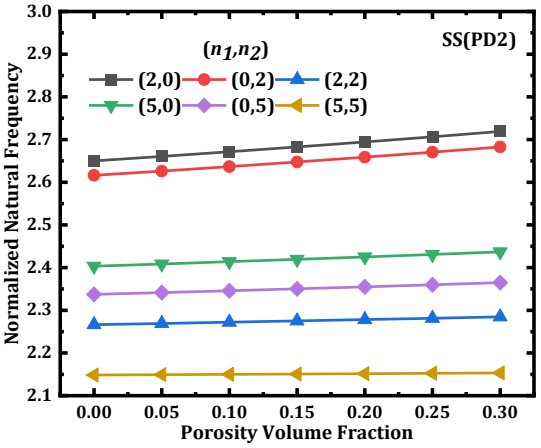

Fig. 9b. Effect of porosity volume fraction on the normalized natural frequency of simply-supported (SS) BDFG plates with non-uniform porosity distribution

3.2.2. Influence of radius to thickness ratio

The effect of radius to thickness ratio (a/h) on normalized natural frequencies of BDFG porous circular plate with clamped and simply-supported boundary conditions are shown in Fig. 10(a-b). In the parametric study, values of the material grading index in thickness (n_1) and radial (n_2) direction are taken as (n_1,n_2) = (1,0), (0,1), (1,1) and the value of porosity volume fraction is taken as (δ) =0.2. The circular BDFG porous plate is made up of material 1.

It is observed that fundamental frequencies increase with radius to thickness ratio (a/h), but no noticeable variation exceeds (a/h) =20. Again, fundamental frequencies for porous BDFG plates considering both boundary conditions, are lower than unidirectional FGMs.

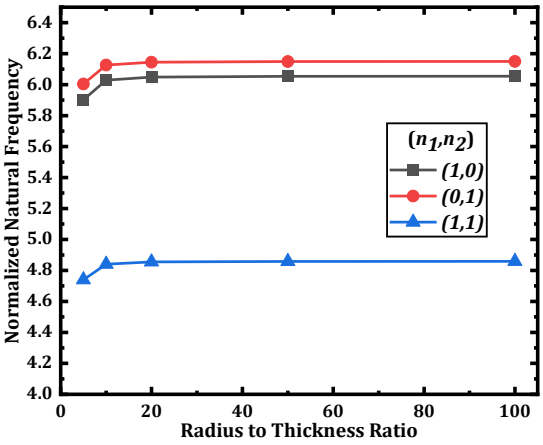

Fig. 10a. Effect of radius to thickness ratio (a/h) on normalized natural frequencies of porous BDFG plates for clamped boundary condition

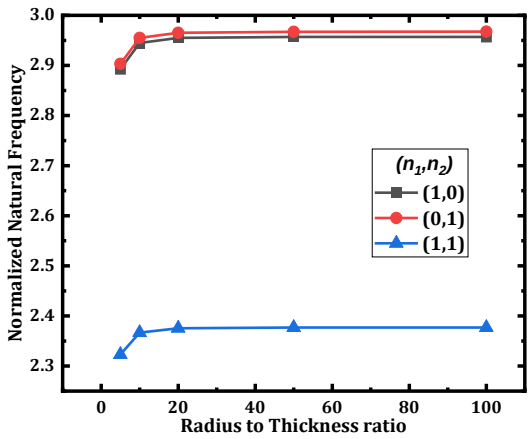

Fig. 10b. Effect of radius to thickness ratio on the normalized natural frequency of porous BDFG plates for simply supported boundary condition

3.2.3. Influence of different material grading indexes

Table 4 shows the effect of different material grading indexes in the thickness direction(n_1) on normalized natural frequencies of clamped circular and annular plates considering uniform (PD1) and non-uniform (PD2) porosity distribution. Table 5 shows the effect of different material grading indexes in the radial direction(n_2) on normalized natural frequencies of clamped circular and annular plates considering uniform and non-uniform porosity. Table 6 shows the effect of different material grading indexes on normalized natural frequencies of the clamped BDFG circular and annular plate with grading index in thickness (n_1) and radial direction (n_2). The radius ratio are taken as (b/a) = 0, 0.1, 0.2, 0.3 and 0.5 and the value of radius to thickness ratio is taken as (a/h) = 5. The value of porosity volume fraction is taken as (δ) =0.1 with material 1 for Tables 4-6.

It is seen from Tables 4-6 that normalized natural frequencies increases with the increase in radius ratio(b/a) and decrease with the increase in grading index for both the porosity distribution PD1 and PD2. Furthermore, the natural frequencies of BDFG circular/annular plates are lower than those of unidirectional FG circular/annular plates, and the effect of the grading index on normalised natural frequencies in the radial direction is stronger than the effect of the grading index on normalised natural frequencies in the thickness direction.

3.2.4. Influence of radius ratio

Now the effect of radius ratio (b/a) on normalized natural frequencies of simply supported BDFG porous plate with uniform (PD1) and non-uniform (PD2) porosity distribution are examined and presented in Figs. 11. (a-b). Fig. 11(a) presents the effect of radius ratio on natural frequencies of simply supported BDFG porous plate with uniform (PD1) porosity distribution, whereas Fig. 11(b) presents the non-uniform (PD2) porosity distribution. the radius ratio are taken as (b/a) = 0, 0.1, 0.2, 0.3 and 0.5 and the value of radius to thickness ratio is taken as (a/h) = 5. The value of porosity volume fraction is taken as (δ) =0.1.

It is observed that for both porosity distribution natural frequencies increase with increase in radius ratio and BDFG plates {(n_1, n_2) = (2, 2)} fundamental frequencies is lower than that of unidirectional plates {(n_1, n_2) =(2, 0) or (n_1, n_2) = (0, 2)}. It is observed that in unidirectional FG simply supported porous circular and annular plates, the normalized fundamental frequencies in the thickness direction are more dominant than that of normalized fundamental frequencies in a radial direction.

4. Conclusions

This study used a differential quadrature method for the free vibration characteristics of bi-directional FGM porous circular/Annular plates. To investigate the effect of porosity on the frequency parameter, two porosity distribution models, uniform and non-uniform, were considered. The power-law method changes the grading index of material properties of a bi-directional FGM plate in the radial and thickness directions utilized to determine material property. The influence of material grading index, types of porosity distribution, porosity volume fraction, aspect ratios, and boundary conditions over normalized frequency of bi-directional FGM porous pate have also been examined. The conclusions of this numerical analysis can be written as follows:

1. The present solution technique is simple, with a fast computational speed with good accuracy.

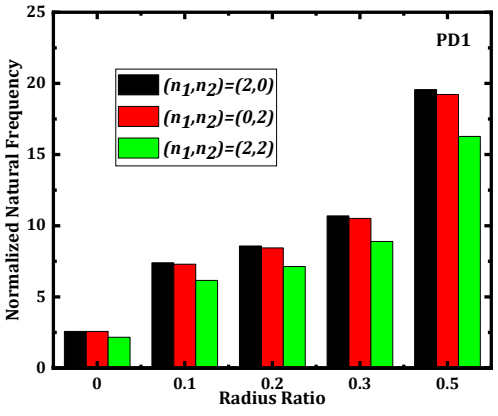

Fig. 11a. Effect of radius ratio on fundamental frequencies of simply supported BDFGs circular and annular plates with uniform porosity distribution

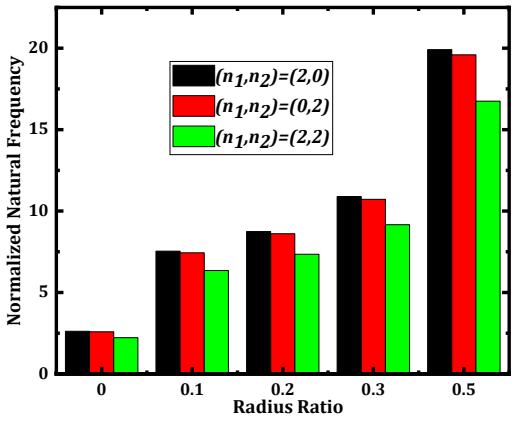

Fig. 11b. Effect of radius ratio on fundamental frequencies of simply supported BDFGs circular and annular plates with non-uniform porosity distribution

2. The natural frequency decrease with an increase in porosity volume fraction for uniform porosity distribution, whereas for non-uniform porosity distribution, the normalized natural frequency increase with the increase in porosity volume fraction for non-uniform porosity distribution.
3. The natural frequency increases with increasing (n_1 and n_2) of BDFG plates for both boundary conditions.
4. The normalized natural frequencies increase with the increase in radius ratio(b/a) and decrease with the increase in grading index for uniform and non-uniform porosity distribution PD1 and PD2.
5. The natural frequencies increase with the radius to thickness ratio (a/h), but no noticeable variation exceeds (a/h) =20.
6. The normalized natural frequencies increased with the increase in radius ratio(b/a) and decreased with an increase in grading index for both the porosity distribution PD1 and PD2.

The aforementioned free vibration response may be served as a benchmark for further investigating the BDFGM plates.

5. References

[1] Ebrahimi, F. and Rastgo, A., 2008. An analytical study on the free vibration of smart circular thin FGM plate based on classical plate theory. *Thin-Walled Structures*, 46(12), pp.1402–1408.

[2] Allahverdizadeh, A., Naei, M.H. and Nikkhah Bahrami, M., 2008. Nonlinear free and forced vibration analysis of thin circular functionally graded plates. *Journal of Sound and Vibration*, 310(4), pp.966–984.

[3] Wirowski, A., 2009. Free vibrations of thin annular plates made from functionally graded material. *PAMM*, 9(1), pp.261–262.

[4] Alipour, M.M., Shariyat, M. and Shaban, M., 2010. A semi-analytical solution for free vibration of variable thickness two-directional-functionally graded plates on elastic foundations. *International Journal of Mechanics and Materials in Design*, 6(4), pp.293–304.

[5] Shariyat, M. and Alipour, M.M., 2011. Differential transform vibration and modal stress analyses of circular plates made of two-directional functionally graded materials resting on elastic foundations. *Archive of Applied Mechanics*, 81(9), pp.1289–1306.

[6] Hamzehkolaei, N.S., Malekzadeh, P. and Vaseghi, J., 2011. Thermal effect on axisymmetric bending of functionally graded circular and annular plates using DQM. *Steel and Composite Structures*, 11(4), pp.341–358.

[7] Liu, Y., Qin, Z. and Chu, F., 2021a. Nonlinear dynamic responses of sandwich functionally graded porous cylindrical shells embedded in elastic media under 1:1 internal resonance. *Applied Mathematics and Mechanics*, 42(6), pp.805–818.

[8] Liu, Y., Qin, Z. and Chu, F., 2021b. Nonlinear forced vibrations of functionally graded piezoelectric cylindrical shells under electric-thermo-mechanical loads. *International Journal of Mechanical Sciences*, 201, p.106474.

[9] Chu, F., Wang, L., Zhong, Z. and He, J., 2014. Hermite radial basis collocation method for vibration of functionally graded plates with in-plane material inhomogeneity. *Computers & Structures*, 142, pp.79–89.

[10] Lal, R. and Ahlawat, N., 2015a. Axisymmetric vibrations and buckling analysis of functionally graded circular plates via differential transform method. *European Journal of Mechanics - A/Solids*, 52, pp.85–94.

[11] Li, S.-R., Wang, X. and Batra, R.C., 2015. Correspondence Relations Between Deflection, Buckling Load, and Frequencies of Thin Functionally Graded Material Plates and Those of Corresponding Homogeneous Plates. *Journal of Applied Mechanics*, [online] 82(11).

[12] Yin, S., Yu, T., Bui, T.Q., Zheng, X. and Yi, G., 2017. Rotation-free isogeometric analysis of functionally graded thin plates considering in-plane material inhomogeneity. *Thin-Walled Structures*, 119, pp.385–395.

[13] Lal, R. and Ahlawat, N., 2015b. Buckling and Vibration of Functionally Graded Non-Uniform Circular Plates Resting On Winkler Foundation. *Latin American Journal of Solids and Structures*, 12(12), pp.2231–2258.
[14] Swaminathan, K., Naveenkumar, D.T., Zenkour, A.M. and Carrera, E., 2015. Stress, vibration and buckling analyses of FGM plates—A state-of-the-art review. *Composite Structures*, 120, pp.10–31.
[15] Merazi, M., Hadji, L., Daouadji, T.H., Tounsi, A. and Bedia, E.A.A., 2015. A new hyperbolic shear deformation plate theory for static analysis of FGM plate based on neutral surface position. *Geomechanics and Engineering*, 8(3), pp.305–321.
[16] Arefi, M., 2015. The effect of different functionalities of FGM and FGPM layers on free vibration analysis of the FG circular plates integrated with piezoelectric layers. *Smart Structures and Systems*, 15(5), pp.1345–1362.
[17] Wu, C.-P. and Liu, Y.-C., 2016. A state space meshless method for the 3D analysis of FGM axisymmetric circular plates. *Steel and Composite Structures*, 22(1), pp.161–182.
[18] Żur, K.K., 2018. Quasi-Green's function approach to free vibration analysis of elastically supported functionally graded circular plates. *Composite Structures*, 183, pp.600–610.
[19] Baltac, A.K., 2018. Numerical approaches for vibration response of annular and circular composite plates. *Steel and Composite Structures*, 29(6), pp.759–770.
[20] Wu, C.-P. and Yu, L.-T., 2018. Quasi-3D static analysis of two-directional functionally graded circular plates. *Steel and Composite Structures*, 27(6), pp.789–801.
[21] Arshid, E., Kiani, A., Amir, S. and Zarghami Dehaghani, M., 2019. Asymmetric free vibration analysis of first-order shear deformable functionally graded magneto-electro-thermo-elastic circular plates. *Proceedings of the Institution of Mechanical Engineers, Part C: Journal of Mechanical Engineering Science*, 233(16), pp.5659–5675.
[22] Javani, M., Kiani, Y. and Eslami, M.R., 2021. Geometrically nonlinear free vibration of FG-GPLRC circular plate on the nonlinear elastic foundation. *Composite Structures*, 261, p.113515.
[23] Singh, P.P. and Azam, M.S., 2021. Buckling and free vibration characteristics of embedded inhomogeneous functionally graded elliptical plate in hygrothermal environment. *Proceedings of the Institution of Mechanical Engineers, Part L: Journal of Materials: Design and Applications*, 235(5), pp.1046–1065.
[24] Kumar, R., Lal, A., Singh, B.N. and Singh, J., 2020. Nonlinear analysis of porous elastically supported FGM plate under various loading. *Composite Structures*, 233, p.111721.
[25] Mouaici, F., Benyoucef, S., Atmane, H.A. and Tounsi, A., 2016. Effect of porosity on vibrational characteristics of non-homogeneous plates using hyperbolic shear deformation theory. *Wind & structures*, 22(4), pp.429–454.
[26] Akbaş, Ş.D., 2017. Vibration and Static Analysis of Functionally Graded Porous Plates. *Journal of Applied and Computational Mechanics*, 3(3), pp.199–207.
[27] M C, K. and Kattimani, S.C., 2018. Assessment of porosity influence on vibration and static behaviour of functionally graded magneto-electro-elastic plate: A finite element study. *European Journal of Mechanics - A/Solids*, 71.
[28] Barati, M.R. and Zenkour, A.M., 2018. Electro-thermoelastic vibration of plates made of porous functionally graded piezoelectric materials under various boundary conditions. *Journal of Vibration and Control*, 24(10), pp.1910–1926.
[29] Zhao, J., Choe, K., Xie, F., Wang, A., Shuai, C. and Wang, Q., 2018. Three-dimensional exact solution for vibration analysis of thick functionally graded porous (FGP) rectangular plates with arbitrary boundary conditions. *Composites Part B: Engineering*, 155, pp.369–381.
[30] Yousfi, M., Atmane, H.A., Meradjah, M., Tounsi, A. and Bennai, R., 2018. Free vibration of FGM plates with porosity by a shear deformation theory with four variables. *Structural Engineering and Mechanics*, 66(3), pp.353–368.
[31] Slimane, M., 2019. Free Vibration Analysis of Composite Material Plates' Case of a Typical Functionally Graded FG Plates Ceramic/Metal' with Porosities. *Nano Hybrids and Composites*, 25, pp.69–83.
[32] Demirhan, P.A. and Taskin, V., 2019. Bending and free vibration analysis of Levy-type porous functionally graded plate using state space approach. *Composites Part B: Engineering*, 160, pp.661–676.
[33] Ali, Md.I. and Azam, M.S., 2021. Exact solution by dynamic stiffness method for the natural vibration of porous functionally graded plate considering neutral surface. *Proceedings of the Institution of Mechanical Engineers, Part L: Journal of Materials: Design and Applications*, 235(7), pp.1585–1603.

[34] Xue, Y., Jin, G., Ma, X., Chen, H., Ye, T., Chen, M. and Zhang, Y., 2019. Free vibration analysis of porous plates with porosity distributions in the thickness and in-plane directions using isogeometric approach. *International Journal of Mechanical Sciences*, 152, pp.346–362.

[35] Hadji, L., Bernard, F., Safa, A. and Tounsi, A., 2021. Bending and free vibration analysis for FGM plates containing various distribution shape of porosity. *Advances in Materials Research*, 10(2), pp.115–135.

[36] Kumar, R., Lal, A., Singh, B.N. and Singh, J., 2019. Meshfree approach on buckling and free vibration analysis of porous FGM plate with proposed IHHSDT resting on the foundation. *Curved and Layered Structures*, 6(1), pp.192–211.

[37] Solanki, M.K., Kumar, R. and Singh, J., 2018. Flexure analysis of laminated plates using multiquadratic RBF based meshfree method. *International Journal of Computational Methods*, 15(06), p.1850049.

[38] Singh, S. and Harsha, S., 2021. Analysis of porosity effect on free vibration and buckling responses for sandwich sigmoid function based functionally graded material plate resting on Pasternak foundation using Galerkin Vlasov's method. *Journal of Sandwich Structures & Materials*, 23(5), pp.1717–1760.

[39] Balak, M., Mehrabadi, S.J., Monfared, H.M. and Feizabadi, H., 2021. Free vibration analysis of a composite elliptical plate made of a porous core and two piezoelectric layers. *Proceedings of the Institution of Mechanical Engineers, Part L: Journal of Materials: Design and Applications*, 235(4), pp.796–812.

[40] Bansal, G., Gupta, A. and Katiyar, V., 2020. Vibration of porous functionally graded plates with geometric discontinuities and partial supports. *Proceedings of the Institution of Mechanical Engineers, Part C: Journal of Mechanical Engineering Science*, 234(21), pp.4149–4170.

[41] Van Vinh, P. and Huy, L.Q., 2022. Finite element analysis of functionally graded sandwich plates with porosity via a new hyperbolic shear deformation theory. *Defence Technology*, 18(3), pp.490–508.

[42] Arshid, E. and Khorshidvand, A.R., 2018. Free vibration analysis of saturated porous FG circular plates integrated with piezoelectric actuators via differential quadrature method. *Thin-Walled Structures*, 125, pp.220–233.

[43] Żur, K.K. and Jankowski, P., 2018. Exact Analytical Solution for Free Axisymmetric and Non-Axisymmetric Vibrations of FGM Porous Circular Plates. [online]

[44] Arshid, E., Khorshidvand, A.R. and Khorsandijou, S.M., 2019. The effect of porosity on free vibration of SPFG circular plates resting on visco-Pasternak elastic foundation based on CPT, FSDT and TSDT. *Structural Engineering and Mechanics*, 70(1), pp.97–112.

[45] Żur, K.K. and Jankowski, P., 2019. Multiparametric Analytical Solution for the Eigenvalue Problem of FGM Porous Circular Plates. *Symmetry*, 11(3), p.429.

[46] Emdadi, M., Mohammadimehr, M. and Navi, B.R., 2019. Free vibration of an annular sandwich plate with CNTRC facesheets and FG porous cores using Ritz method. *Advances in Nano Research*, 7(2), pp.109–123.

[47] Van Vinh, P. and Tounsi, A., 2022. Free vibration analysis of functionally graded doubly curved nanoshells using nonlocal first-order shear deformation theory with variable nonlocal parameters. *Thin-Walled Structures*, 174, p.109084.

[48] Heshmati, M. and Jalali, S.K., 2019. Effect of radially graded porosity on the free vibration behavior of circular and annular sandwich plates. *European Journal of Mechanics - A/Solids*, 74, pp.417–430.

[49] Amir, S., Arshid, E. and Arani, M.R.G., 2019. Size-dependent magneto-electro-elastic vibration analysis of FG saturated porous annular/ circular micro sandwich plates embedded with nano-composite face sheets subjected to multi-physical pre loads. *Smart Structures and Systems*, 23(5), pp.429–447.

[50] Bennai, R., Atmane, H.A., Ayache, B., Tounsi, A., Bedia, E.A.A. and Al-Osta, M.A., 2019. Free vibration response of functionally graded Porous plates using a higher-order Shear and normal deformation theory. *Earthquakes and Structures*, 16(5), pp.547–561.

[51] Gao, W., Qin, Z. and Chu, F., 2020. Wave propagation in functionally graded porous plates reinforced with graphene platelets. *Aerospace Science and Technology*, 102, p.105860.

[52] Kumar, R. and Singh, J., 2018. Assessment of higher order transverse shear deformation theories for modeling and buckling analysis of FGM plates using RBF based meshless approach. *Multidiscipline Modeling in Materials and Structures*.

[53] Kaddari, M., Kaci, A., Bousahla, A.A., Tounsi, A., Bourada, F., AbdeldjebbarTounsi, Bedia, E.A.A. and Al-Osta, M.A., 2020. A study on the structural behaviour of functionally graded

porous plates on elastic foundation using a new quasi-3D model: Bending and free vibration analysis. *Computers and Concrete*, 25(1), pp.37–57.

[54] Safarpour, M., Rahimi, A., Alibeigloo, A., Bisheh, H. and Forooghi, A., 2021. Parametric study of three-dimensional bending and frequency of FG-GPLRC porous circular and annular plates on different boundary conditions. *Mechanics Based Design of Structures and Machines*, 49(5), pp.707–737.

[55] Shojaeefard, M., Saeidi, H., Ghadiri, M. and Mahinzare, M., 2017. Micro temperature-dependent FG porous plate: Free vibration and thermal buckling analysis using modified couple stress theory with CPT and FSDT. *Applied Mathematical Modelling*, 50.

[56] Thom, D., Nguyen, D., Duc, N., Doan, H.D. and Bui, T.Q., 2017. Analysis of bi-directional functionally graded plates by FEM and a new third-order shear deformation plate theory. *Thin-Walled Structures*, 119, pp.687–699.

[57] Lieu, Q.X., Lee, D., Kang, J. and Lee, J., 2019. NURBS-based modeling and analysis for free vibration and buckling problems of in-plane bi-directional functionally graded plates. *Mechanics of Advanced Materials and Structures*, 26(12), pp.1064–1080.

[58] Lieu, Q.X., Lee, S., Kang, J. and Lee, J., 2018. Bending and free vibration analyses of in-plane bi-directional functionally graded plates with variable thickness using isogeometric analysis. *Composite Structures*, 192.

[59] Hong, N., 2020. Nonlinear Static Bending and Free Vibration Analysis of Bidirectional Functionally Graded Material Plates. *International Journal of Aerospace Engineering*, 2020, pp.1–16.

[60] Vinh, P.V., 2021. Analysis of bi-directional functionally graded sandwich plates via higher-order shear deformation theory and finite element method. *Journal of Sandwich Structures & Materials*, p.10996362211025812.

[61] Van Vinh, P., 2021. Deflections, stresses and free vibration analysis of bi-functionally graded sandwich plates resting on Pasternak's elastic foundations via a hybrid quasi-3D theory. *Mechanics Based Design of Structures and Machines*, 0(0), pp.1–32.

[62] Jin, G., Ye, T., Ma, X., Chen, Y., Su, Z. and Xie, X., 2013. A unified approach for the vibration analysis of moderately thick composite laminated cylindrical shells with arbitrary boundary conditions. *International Journal of Mechanical Sciences*, 75, pp.357–376.

[63] Su, Z., Jin, G., Shi, S., Ye, T. and Jia, X., 2014. A unified solution for vibration analysis of functionally graded cylindrical, conical shells and annular plates with general boundary conditions. *International Journal of Mechanical Sciences*, 80, pp.62–80.

[64] Qin, Z., Chu, F. and Zu, J., 2017. Free vibrations of cylindrical shells with arbitrary boundary conditions: A comparison study. *International Journal of Mechanical Sciences*, 133, pp.91–99.

[65] Qin, Z., Yang, Z., Zu, J. and Chu, F., 2018. Free vibration analysis of rotating cylindrical shells coupled with moderately thick annular plates. *International Journal of Mechanical Sciences*, 142–143, pp.127–139.

[66] Qin, Z., Pang, X., Safaei, B. and Chu, F., 2019. Free vibration analysis of rotating functionally graded CNT reinforced composite cylindrical shells with arbitrary boundary conditions. *Composite Structures*, 220,

[67] Qin, Z., Zhao, S., Pang, X., Safaei, B. and Chu, F., 2020. A unified solution for vibration analysis of laminated functionally graded shallow shells reinforced by graphene with general boundary conditions. *International Journal of Mechanical Sciences*, 170, p.105341.

[68] Shariyat, M. and Alipour, M.M., 2013. A power series solution for vibration and complex modal stress analyses of variable thickness viscoelastic two-directional FGM circular plates on elastic foundations. *Applied Mathematical Modelling*, 37(5), pp.3063–3076.

[69] Tahouneh, V., 2014. Free vibration analysis of bidirectional functionally graded annular plates resting on elastic foundations using differential quadrature method. *Structural Engineering & Mechanics*, 52, p.663.

[70] Lal, R. and Ahlawat, N., 2017. Buckling and vibrations of two-directional functionally graded circular plates subjected to hydrostatic in-plane force. *Journal of Vibration and Control*, 23(13), pp.2111–2127.

[71] Mahinzare, M., Ranjbarpur, H. and Ghadiri, M., 2018. Free vibration analysis of a rotary smart two directional functionally graded piezoelectric material in axial symmetry circular nanoplate. *Mechanical Systems and Signal Processing*, 100, pp.188–207.

[72] Shojaeefard, M.H., Saeidi Googarchin, H., Mahinzare, M. and Ghadiri, M., 2018. Free vibration and critical angular velocity of a rotating variable thickness two-directional FG circular microplate. *Microsystem Technologies*, 24(3), pp.1525–1543.

[73] Ahlawat, N., 2019. Numerical solution for buckling and vibration of bi-directional FGM circular plates. *AIP Conference Proceedings*, 2061(1), p.020020.

[74] Molla-Alipour, M., Shariyat, M. and Shaban, M., 2020. Free Vibration Analysis of Bidirectional Functionally Graded Conical/Cylindrical Shells and Annular Plates on Nonlinear Elastic Foundations, Based on a Unified Differential Transform Analytical Formulation. *Journal of Solid Mechanics*, 12(2), pp.385–400.

[75] Bert, C.W. and Malik, M., 1997. Differential quadrature: a powerful new technique for analysis of composite structures. *Composite Structures*, 39(3), pp.179–189.

[76] Jiang, W. and Redekop (Canada), D., 2002. Analysis of transversely isotropic hollow toroids using the semi-analytical DQM. *Structural Engineering and Mechanics*, 13(1), pp.103–116.

[77] Ferreira, A., Carrera, E., Cinefra, M., Viola, E., Tornabene, F., Fantuzzi, N. and Zenkour, A., 2014. Analysis of Thick Isotropic and Cross-Ply Laminated Plates by Generalized Differential Quadrature Method and a Unified Formulation. *Composites Part B Engineering*, 58, pp.544–552.

[78] Alibeigloo, A. and Alizadeh, M., 2015. Static and free vibration analyses of functionally graded sandwich plates using state space differential quadrature method. *European Journal of Mechanics - A/Solids*, 54, pp.252–266.

[79] Arani, A.G., Khoddami Maraghi, Z., Khani, M. and Alinaghian, I., 2017. Free Vibration of Embedded Porous Plate Using Third-Order Shear Deformation and Poroelasticity Theories. *Journal of Engineering*, 2017, p.e1474916.

[80] Nejati, M., Fard, K.M., Eslampanah, A. and Jafari, S.S., 2017. Free Vibration Analysis of Reinforced Composite Functionally Graded Plates with Steady State Thermal Conditions. *Latin American Journal of Solids and Structures*, 14, pp.886–905.

[81] Ji, C., Yao, L., Shen, J., Hu, T. and Li, C., 2019. In-Plane Free Vibration of Functionally Graded Rectangular Plates with Elastic Restraint. *Global Journal of Engineering Sciences*, 2(3), pp.1–8.

[82] Civalek, O. and Ulker, M., 2004. Harmonic differential quadrature (HDQ) for axisymmetric bending analysis of thin isotropic circular plates. *Structural Engineering and Mechanics*, 17(1), pp.1–14.

[83] Mirtalaie, S.H. and Hajabasi, M.A., 2011. Free vibration analysis of functionally graded thin annular sector plates using the differential quadrature method. *Proceedings of the Institution of Mechanical Engineers, Part C: Journal of Mechanical Engineering Science*, 225(3), pp.568–583.

[84] Mirtalaie, S., Hajabbasi, M. and Hejripour, F., 2011. Free Vibration Analysis of Functionally Graded Moderately Thick Annular Sector Plates Using Differential Quadrature Method. *Proceedings of the Institution of Mechanical Engineers, Part C: Journal of Mechanical Engineering Science*, 225.

[85] Jodaei, A., Jalal, M. and Yas, M.H., 2012. Free vibration analysis of functionally graded annular plates by state-space based differential quadrature method and comparative modeling by ANN. *Composites Part B: Engineering*, 43(2), pp.340–353.

[86] Ahlawat, N. and Lal, R., 2016. Buckling and Vibrations of Multi-directional Functionally Graded Circular Plate Resting on Elastic Foundation. *Procedia Engineering*, 144, pp.85–93.

[87] Shahriari, B., Jalali, M. and Karamooz Ravari, M., 2017. Vibration analysis of a rotating variable thickness bladed disk for aircraft gas turbine engine using generalized differential quadrature method. *Proceedings of the Institution of Mechanical Engineers, Part G: Journal of Aerospace Engineering*, 231(14), pp.2739–2749.

[88] Mohammadimehr, M., Afshari, H., Salemi, M., Torabi, K. and Mehrabi, M., 2019. Free vibration and buckling analyses of functionally graded annular thin sector plate in-plane loads using GDQM. *Structural Engineering and Mechanics*, 71(5), pp.525–544.

[89] Lal, R. and Saini, R., 2020. Vibration analysis of functionally graded circular plates of variable thickness under thermal environment by generalized differential quadrature method. *Journal of Vibration and Control*, 26(1–2), pp.73–87.

[90] Behravan Rad, A., 2018. Static analysis of non-uniform 2D functionally graded auxetic-porous circular plates interacting with the gradient elastic foundations involving friction force. *Aerospace Science and Technology*, 76, pp.315–339.

[91] Li, S., Zheng, S. and Chen, D., 2020. Porosity-dependent isogeometric analysis of bi-directional functionally graded plates. *Thin-Walled Structures*, 156, p.106999.

[92] Shariyat, M. and Jafari, R., 2013. A micromechanical approach for semi-analytical low-velocity impact analysis of a bidirectional functionally graded circular plate resting on an elastic foundation. *Meccanica*, 48(9), pp.2127–2148.

[93] Akbari, P. and Asanjarani, A., 2019. Semi-analytical mechanical and thermal buckling analyses of 2D-FGM circular plates based on the FSDT. *Mechanics of Advanced Materials and Structures*, 26(9), pp.753–764.

[94] Reddy, J.N., 2003. Mechanics of Laminated Composite Plates and Shells: Theory and Analysis*, Second Edition*. CRC Press.

[95] Yin, S., Hale, J.S., Yu, T., Bui, T.Q. and Bordas, S.P.A., 2014. Isogeometric locking-free plate element: A simple first order shear deformation theory for functionally graded plates. *Composite Structures*, 118, pp.121–138.

[96] Bellman, R., Kashef, B.G. and Casti, J., 1972. Differential quadrature: A technique for the rapid solution of nonlinear partial differential equations. *Journal of Computational Physics*, 10(1), pp.40–52.

[97] Khare, S. and Mittal, N.D., 2019. Axisymmetric bending and free vibration of symmetrically laminated circular and annular plates having elastic edge constraints. *Ain Shams Engineering Journal*, 10(2), pp.343–352.